Adsorption (2024) 30:651–661
https://doi.org/10.1007/s10450-024-00452-z

Coupling effect of temperature, column height, properties of adsorbent and VOCs during dynamic adsorption

Lijuan Jia[1] · Mingxuan Yang[1] · Xiangbin Shen[1] · Yangping Zhang[1] · Dan Luo[1] · Yuying Zhang[1]

Received: 16 November 2023 / Revised: 13 March 2024 / Accepted: 14 March 2024 / Published online: 6 April 2024

Abstract
Dynamic adsorption is important for evaluating the Volatile Organic Compounds (VOCs) adsorption performance. During adsorption process, the exothermal characteristic could lead to an increase of the column temperature, which might cause bed combustion and is negative to the adsorption efficiency. In present study, we chose graphene oxide(GO) as adsorbent, comparing with hypercrosslinked polymeric adsorbent(HPA), and conducted the dynamic adsorption experiment of ethanol, n-hexane and cyclohexane at 308 K, 318 and 328 K with different adsorbent column height. The results showed that the temperature had linear and negative influence on breakthrough capacity for three VOCs on two adsorbents. And the breakthrough adsorption capacity of ethanol, n-hexane and cyclohexane on two adsorbents were as follows: ethanol > cyclohexane > n-hexane, closely related with physical parameters of VOCs. But the physical properties of ethanol, n-hexane and cyclohexane have little influence on dynamic adsorption rate in this paper. In addition, for n-hexane and cyclohexane, the breakthrough adsorption capacity on HPA were higher than that on GO, but their k values were similarity on HPA and GO. While for ethanol, the breakthrough capacity and k value on GO were higher than HPA. Most important of all, the negative effect of temperature on VOCs adsorption on GO was lower than HPA. Therefore, GO is a good alternative adsorbent for VOCs recovery. Furthermore, with higher column height, the dynamic adsorption capacity was higher but the adsorption rate was lower. While the influence of temperature on dynamic adsorption capacity and rate were relative independent with column height of adsorbent.

Keywords Column height · Temperature · VOCs · Hypercrosslinked polymeric adsorbent · Graphene oxide

1 Introduction

Volatile Organic Compounds (VOCs) are the main atmospheric pollutants in recent years [2], which could cause dyspnea, eye and throat irritation, and cancer [31]. Considering the simple design and operation, high selectivity, high adsorption capacity and low-cost for VOCs separation, adsorption method has been broadly considered as a superior technology for VOCs removal [6, 16, 23, 35]. Practically, fixed-bed adsorption is widely adopted in the application of adsorption for VOCs separation and purification, so as to achieve optimum results [13, 17, 24, 29, 30].

The exothermal characteristics during adsorption process could cause high adsorbent column temperature [1]. At high VOCs concentration, the temperature raise could be rather remarkable. Most incidents, coming from fixed-bed combustion, has appeared during the adsorption of aldehydes, ketones and organic sulfides [19, 26]. Because of the poor thermal conductivity of granular adsorbents, performances of gas separation are usually highly weaken by the induced adsorptive thermal effects [27]. The temperature effect on dynamic adsorption behavior of VOCs is worth studying for adsorbent preparation and fixed-bed design, which are the core role during the adsorption process.

In order to improve adsorption performance, it is vital to design a suitable fixed bed and adopt proper adsorbent. In extensive investigations, some traditional adsorbents, such as zeolite, activated carbon, biochar and silica gels,

✉ Lijuan Jia
jialijuan1203@163.com

[1] Shanxi Key Laboratory of Ecological Protection and Resources Utilization of Yuncheng Salt Lake, Department of Applied Chemistry, Yuncheng University, 1155 Fudan West Street, Yuncheng 044000, China

Table 1 Selected properties of HPA [17] and GO

Adsorbents	HPA	GO
$S_{BET}(m^2/g)$	944.4	564.8
$V_{mico}(mL/g)$	0.43	0.16
$V_{meso}(mL/g)$	0.36	0.10
Average pore diameter(nm)	2.73	2.44
-OH (mmol/g)	0.207	0.495
-C = O (mmol/g)	0.124	0.452
-COOH (mmol/g)	0.032	0.104
-COOR (mmol/g)	0.374	0.067
Total acidic (mmol/g)	0.737	1.118

were always adopted for VOCs removal [11, 21, 34]. However, their shortcomings of low thermal conductivity, combustion, inefficient desorption and high regeneration energy consumption, have restricted their practical applications [37]. Hypercrosslinked polymer is a class of organic adsorbents with abundant micropore volume and high specific surface area. In recent years, hypercrosslinked polymer has been considered as a promising substitute to traditional adsorbents for VOCs removal due to its superior physical and chemical properties, adjustable pore structure, and efficient regenerability [8, 10, 14, 17]. Graphene oxide (GO), being the most promising graphene material [20], is also a kind of adsorbent with abundant acidic groups and high specific surface area [7]. With the very thin layer thickness, GO is easy to desorb and regenerate after adsorption and resistant to high temperatures [4, 20, 32]. It is a thermal interface material with great development potential.

In this paper, we choose hypercrosslinked polymeric adsorbent(HPA) and graphene oxide(GO) as adsorbents. Dynamic adsorption experiment of ethanol, n-hexane and cyclohexane at 308 K, 318 and 328 K were conducted. The effect of temperature column height(H) on VOCs dynamic adsorption were analyzed and compared on two adsorbents.

2 Materials and methods

2.1 Materials

The synthetic process of hypercrosslinked polymeric adsorbent (HPA) had been pictured meticulously in our previous paper [15, 25]. The graphene was applied by International graphene innovation conference (2018). Ethanol, n-hexane and cyclohexane were purchased from Yuncheng Chemical Reagent Company, China. The porous texture of HPA and GO were characterized by N_2 adsorption-desorption isotherms data at 77 K. We calculated the specific surface areas(SBET) of HPA and GO using Brunauer–Emmett–Teller (BET) based on the N_2 isotherm data at 77 K [15]. The surface acidic groups were measured using Boehm titration method [5]. The acidic groups on HPA and GO were presented in Table 1.

2.2 Breakthrough experiment

The breakthrough experimental setup could be seen in Fig. 1, which included three sections: VOCs vapor generator, the fixed-bed column holding adsorbent, and gas chromatography (GC9890A, Junqi Instrument Equipment Co., Shanghai, China) with flame-ionization detector. In the first section, as the Fig. 1, the dry nitrogen steam was separated into two flows, being controlled by mass flow controllers. One of the two nitrogen flows passed through the bubble saturator containing liquid VOCs, which was put in a thermostatic water bath to control the temperature at 293 K. Then, this stream containing VOCs was diluted by the other nitrogen flow to gain a set concentration of VOCs onto adsorbent. In the second section, the VOCs with a concentration of 15 mg/L and a stable inlet flow rate of 100 mL/min passed through the adsorbent column (5 mm inner diameter). At the outlet of adsorbent column, the concentration of VOCs was determined by gas chromatography. The

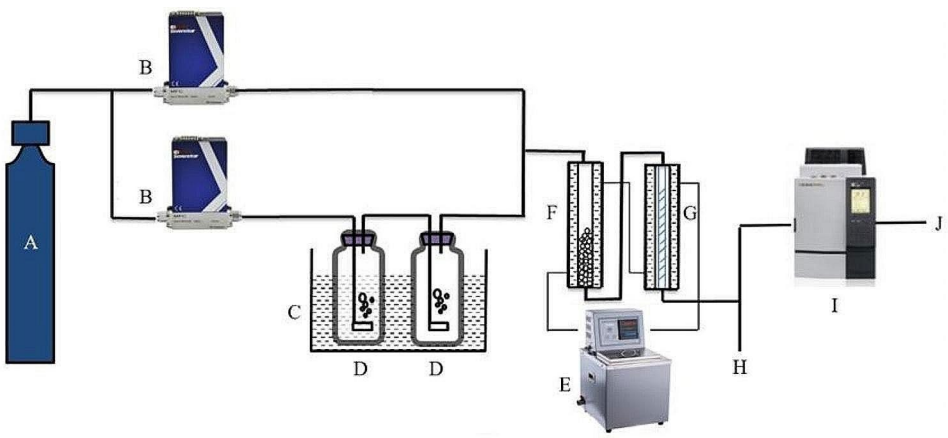

Fig. 1 Column adsorption schematic diagram of VOCs on adsorbents. (A. high purity nitrogen B. mass flow meter C. thermostatic water bath D. VOCs E. circulating water bath F. buffer column G. adsorption column H. offgas I. gas chromatograph J. offgas)

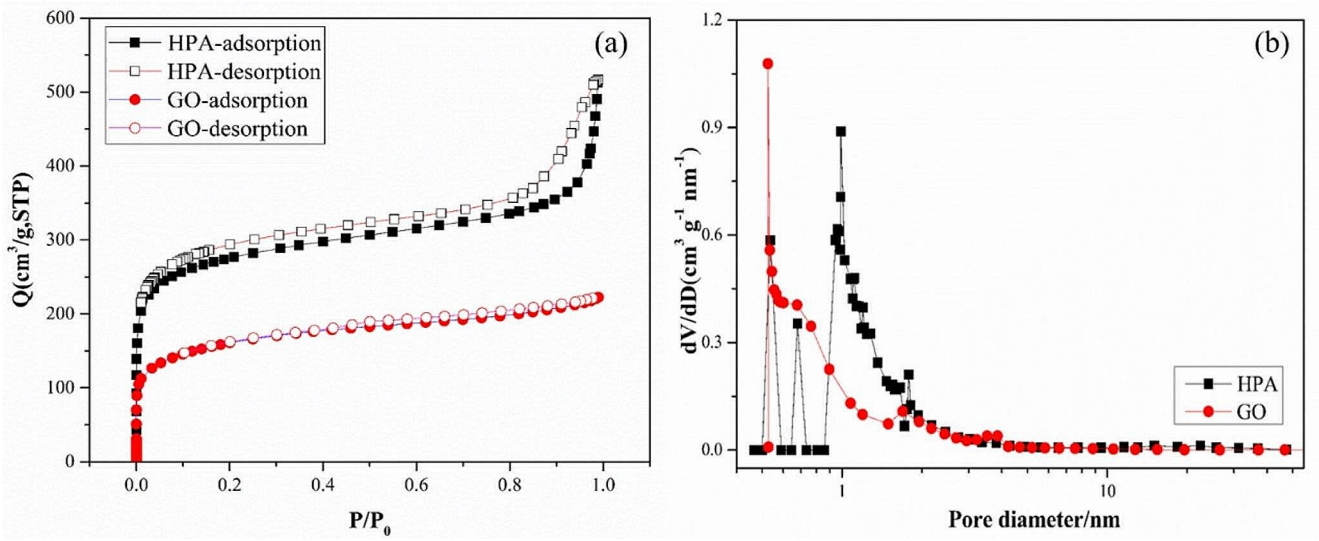

Fig. 2 N_2 adsorption-desorption isotherms at 77 K (a) and pore size distributions (b) of HPA and GO.

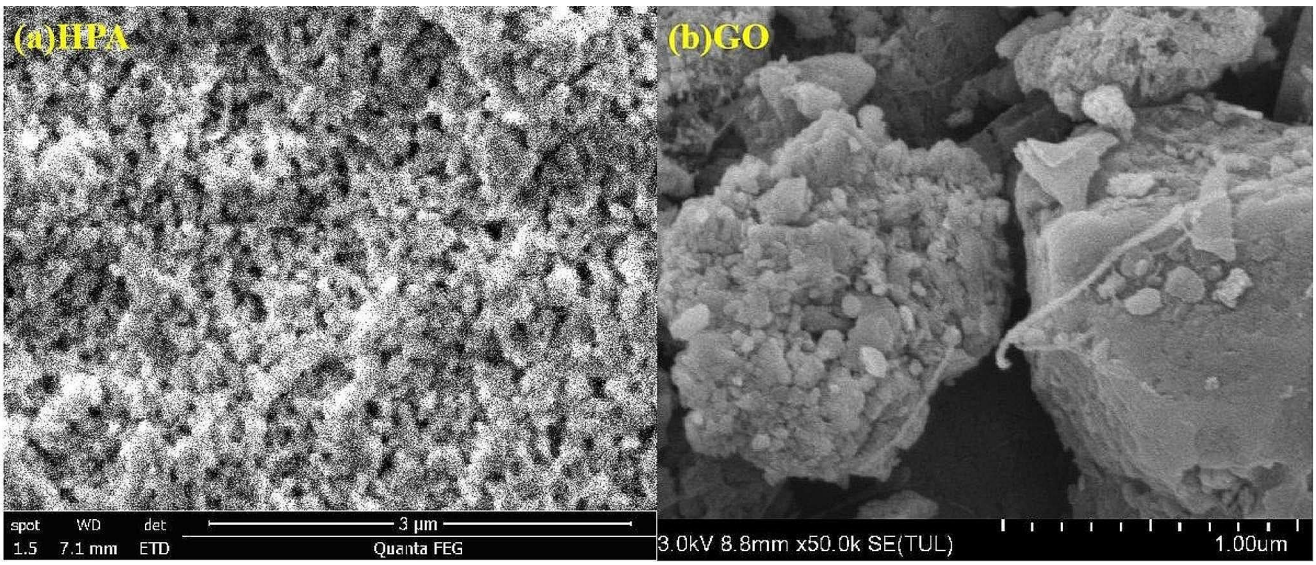

Fig. 3 Scanning Electronic Microscopy (SEM) images of HPA and GO. (a) HPA (b) GO

dynamic adsorption of VOCs were performed at temperatures of 308 K, 318 and 328 K. The height of HPA and GO were set to 5 and 10 cm.

3 Results and discussion

3.1 Characteristic of HPA and GO

It is presented in Fig. 2 that the adsorption amount of nitrogen increased steeply with relative pressure(P/P_0) increasing for P/P_0 below 0.05 on HPA, which has been depicted in detail in our previous paper [17]. This phenomenon could also be observed for GO, indicating that both HPA and GO had abundant micropore. However, at higher $P/P_0(>0.8)$, HPA showed another sharp increase, while the nitrogen uptake on GO reach a plateau, indicating that HPA also had some meso- and macro-pores. The pore size distributions of HPA and GO were displayed in Fig. 2(b) in accordance with Fig. 2(a). The specific surface area of HPA and GO were 944.8m^2/g and 564.8m^2/g, separately.

In order to learn the porous structure of two adsorbents deeply, SEM analysis was done and the results were presented in Fig. 3. SEM image in Fig. 3(a) discerned the abundant mesopores and macropores on HPA. However, it was difficult to visualize micropores on two adsorbents. Combining SEM results and nitrogen adsorption isotherms, the structure of HPA and GO could be learned clearly. That is,

HPA is an adsorbent with micro-, meso- and macro-pores, while GO mainly have considerable micropores.

In addition, the surface chemical nature of HPA and GO were also listed in Table 1. It could be observed clearly that the total amount of acidic groups on GO surface was higher than HPA. This result deduced that GO could form more hydrogen bonds with water vapor or hydrophilic VOCs.

3.2 Breakthrough adsorption capacity of VOCs at different temperatures

To explore the adsorption capacity and behavior of ethanol, n-hexane and cyclohexane at different adsorption temperatures(308 K, 318 and 328 K) on HPA and GO, we conducted dynamic adsorption experiments to clarify the breakthrough adsorption behavior of three VOCs. The experimental results were shown in Figs. 4 and 5. We could learn that the breakthrough time reduced at higher column temperature for three VOCs on HPA and GO. In addition, the breakthrough curves became steeper at higher temperature, meaning higher dynamic adsorption rate. This result indicated the main physic-adsorption mechanism between adsorbent and VOCs, which was widely studied and accepted [3].

To clarify the breakthrough adsorption behavior of ethanol, n-hexane and cyclohexane on HPA and GO quantitatively, the Yoon and Nelson model (Y-N model, Eq. 1)(Yoon and Nelson, [36] was adopted to fit their breakthrough curves.

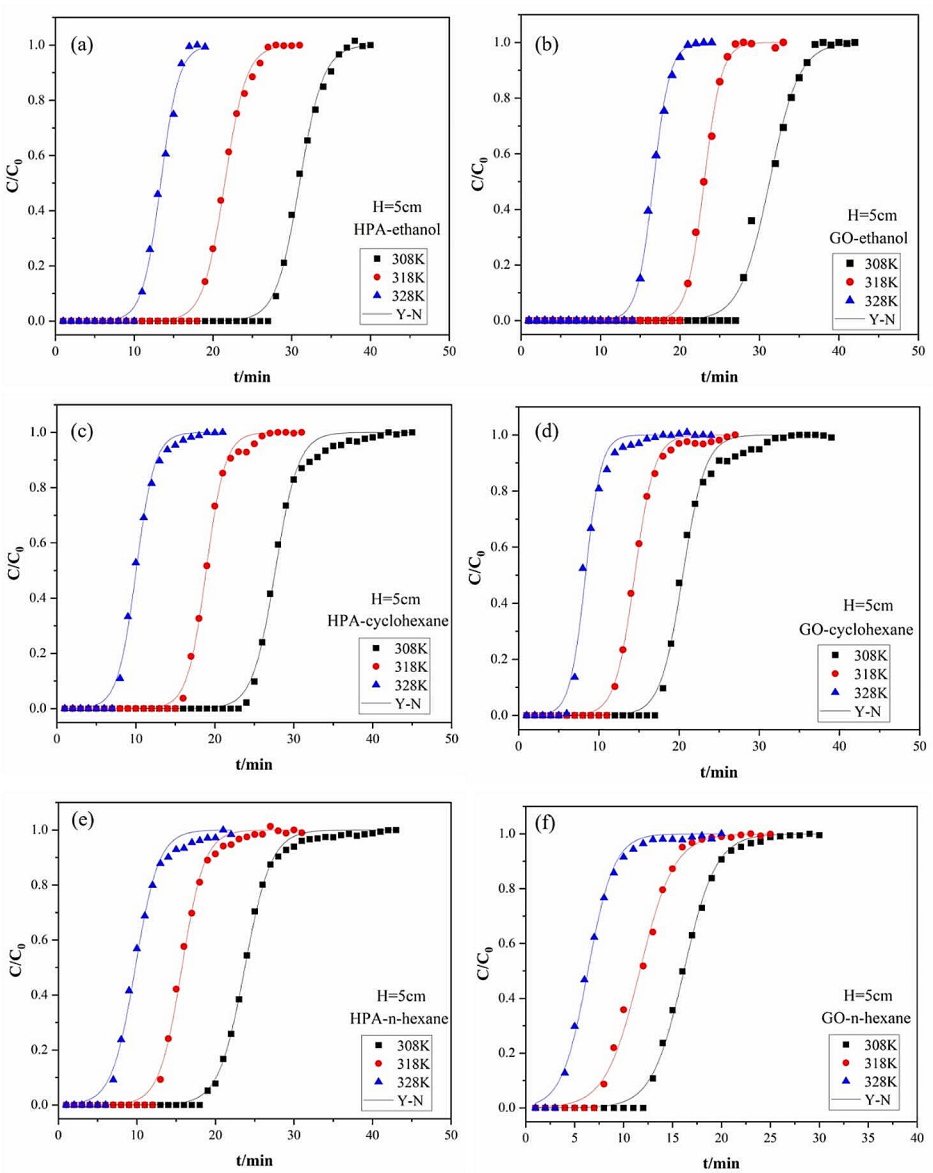

Fig. 4 Breakthrough curves of VOCs on HPA and GO when the column height is 5 cm

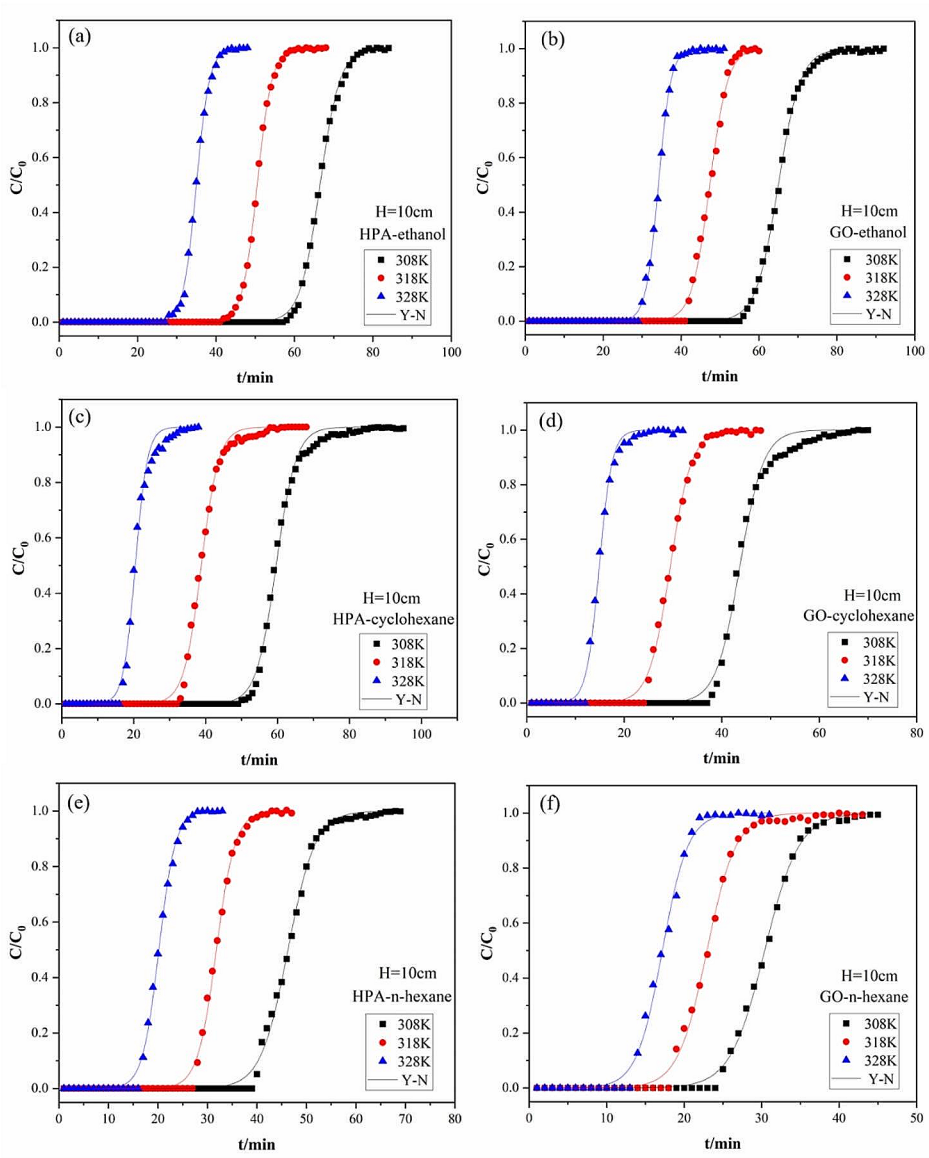

Fig. 5 Breakthrough curves of VOCs on HPA and GO when the column height is 10 cm

$$t = \tau + \frac{1}{k}\ln\frac{C}{C_0 - C} \quad (1)$$

Where t is the breakthrough adsorption time, C_0 and C are inlet and outlet concentrations of VOCs, τ is the time when C/C_0 is 50%, k is the dynamic adsorption rate constant. The Y-N model showed a superior fit to the experimental dynamic adsorption data of three VOCs on HPA and GO with correlation coefficient(R^2) higher than 0.997. In short, the Yoon and Nelson model can describe the entire breakthrough curve in this study, which is beneficial for adsorption process designing. The breakthrough time, when C/C_0 was 5%, was calculated using the fitting results of Y-N equation, shown in Fig. 6. And to further analyze, the breakthrough adsorption capacity were also calculated, presented in Fig. 7.

3.2.1 Effect of VOCs physical properties

It could be noticed from Figs. 6 and 7 that the breakthrough adsorption time and capacity of ethanol, n-hexane and cyclohexane on two adsorbents were as follows: ethanol > cyclohexane > n-hexane. This might be related with physical parameters of VOCs, such as the polarizabilities, molar volumes, saturated pressures or parachors [33]. According to the physical properties of three VOCs, listed in Table 2, we made relationship diagram between breakthrough time of three VOCs and their

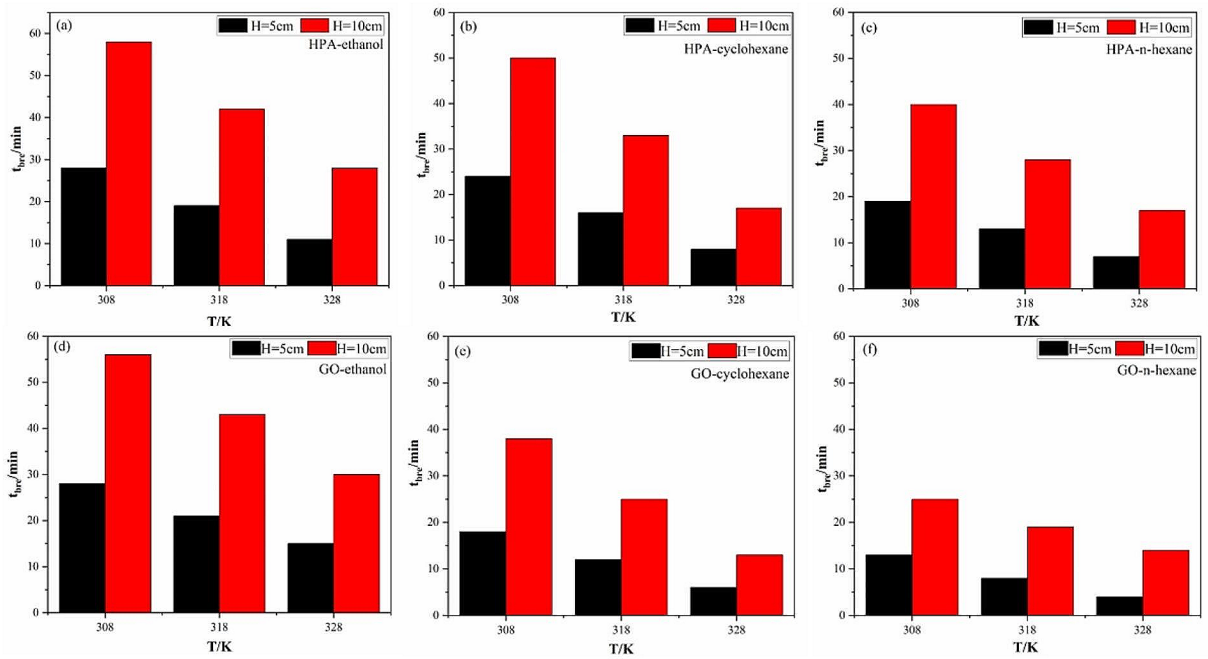

Fig. 6 The breakthrough adsorption time of VOCs on HPA and GO at different temperatures

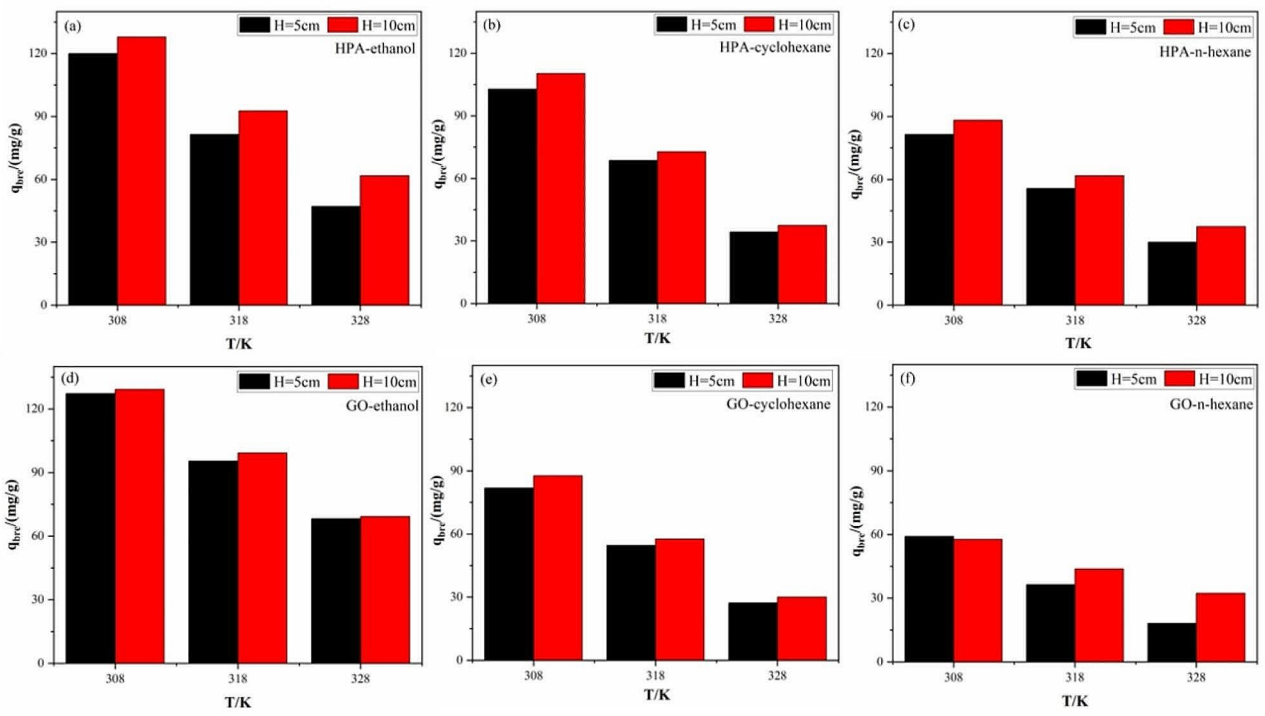

Fig. 7 The breakthrough adsorption capacity of VOCs on HPA and GO at different temperatures

Table 2 The physical-chemical properties of VOCs

VOCs	ethanol	cyclohexane	n-hexane
Molecular weight	46.1	86.2	86.2
Boil point/℃	78.4	68.9	68.9
Molar volume/(cm^3/mol)	59.0	106.4	127.5
Polarizability ($10^{-24}cm^3$)	5.09	10.96	11.83
Saturated pressure/KPa(293 K)	5.8	12.7	17.0
Molecular dynamics diameter(nm)	0.45	0.60	0.43

polarizabilities, molar volumes and saturated pressures, shown in Fig. 8. The results displayed that the saturated pressure and molar volume have better linear relationship with the breakthrough adsorption capacity of three VOCs. This is similar to the relationship between equilibrium adsorption capacity and physical properties of VOCs [18], suggesting that physical adsorption act as a dominant role.

3.2.2 Effect of adsorbent properties

In addition, we could observe from Fig. 7 that for n-hexane and cyclohexane, the breakthrough adsorption capacity on HPA were higher than GO. While for ethanol(seen from Fig. 7(a,d)), the breakthrough adsorption capacity on GO was slightly higher than HPA. Considering the specific surface area, S_{BET} of HPA is higher than GO, indicating that the adsorption performance of HPA may be better than GO, showing similar trend for n-hexane and cyclohexane. For ethanol, the probable interpretation for this phenomenon is that GO has a higher amount of oxygenic groups (Table 1). Ethanol could form hydrogen bond with oxygenic groups, meaning that GO have a higher affinity to ethanol than HPA, contributing to improve the adsorption performance.

To further elucidate the influence of temperature, we make the relationship between temperature and breakthrough adsorption capacity of three VOCs with two

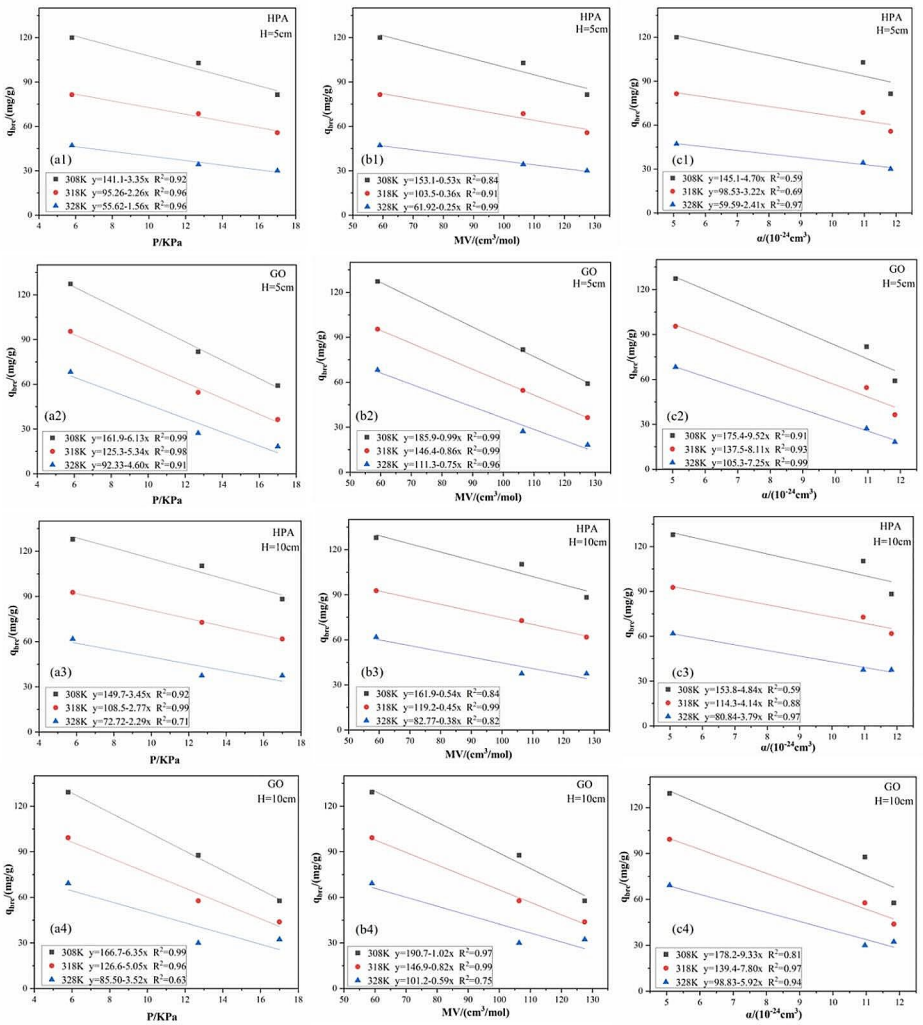

Fig. 8 The relationship between dynamic adsorption capacity and physic-chemical properties of VOCs (a:Saturated pressure/KPa(293 K), b:Molar volume, c:Polarizability)

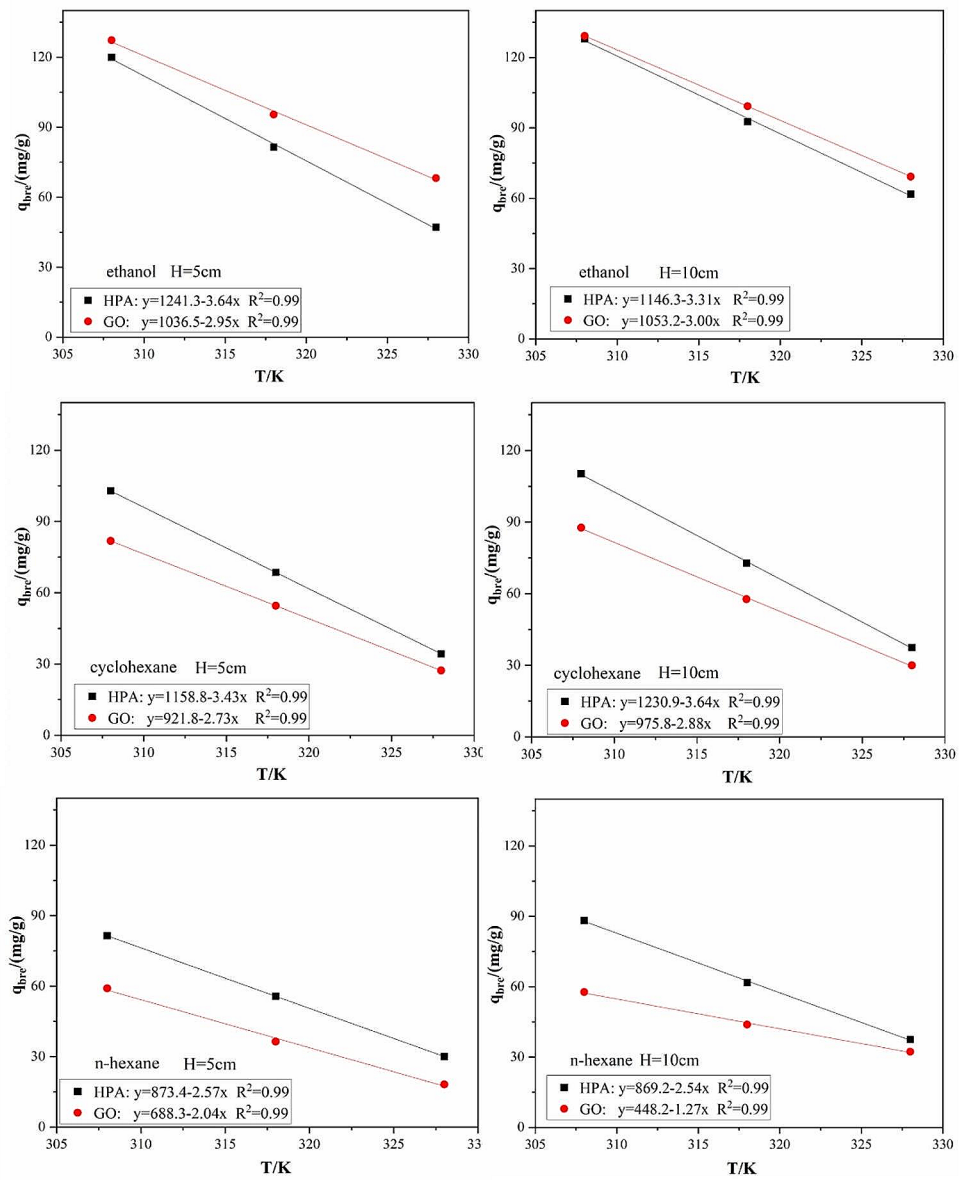

Fig. 9 Linear relationship between breakthrough adsorption capacity of VOCs and temperature with different adsorbent column height

column heights(H = 5 cm and H = 10 cm), as presented in Fig. 9. It was clearly visible that the breakthrough adsorption capacity of three VOCs linearly reduced with temperature increasing, implying that the working adsorption capacity of HPA and GO sharply and linearly decreased with the increase of temperature. From fitting line, it is worth noting that the slopes of GO were slightly lower than those of HPA, indicating that the negative effect of temperature on VOCs adsorption on GO was lower than HPA. This could be attributed to the higher thermal conductivity of GO [4, 32], which is advantageous for weakening the negative influence of temperature.

3.2.3 Effect of column height

Notably, as depicted in Fig. 6, the breakthrough adsorption time for three VOCs at the height of 10 cm in the adsorbent column was found to be more than twice that observed at H = 5 cm that observed at H = 5 cm. The higher the height of fixed-bed column was, the larger the amount of adsorbent in the column was, resulting in that larger surface area and active adsorbent sites were available for VOCs adsorption [28]. In addition, VOCs had longer time to contact with the adsorbent as the column height rose, resulting in higher VOCs elimination [12]. But when we compared the breakthrough adsorption capacity on adsorbent per unit mass, with different column height, as shown in Fig. 7,

it is obviously that the difference between H = 5 cm and H = 10 cm decreased sharply. These results indicated that adsorbent with relative lower column height had similar adsorption performance with higher column height.

Furthermore, by comparing the slope for H = 5 cm and H = 10 cm in Fig. 9, there was no regular trend or definitive results. This might imply that the negative influence of temperature on dynamic adsorption capacity was relative independent with column height of adsorbent.

3.3 Dynamic adsorption rate of three VOCs at different temperatures

Apart from the aforementioned breakthrough adsorption capacity, the slope of breakthrough curves was also a key factor for evaluating the dynamic adsorption performance. It can be seen from Figs. 4 and 5 that the breakthrough curves became steeper with the increase of temperature, but the breakthrough curves converted somewhat flatter with the fixed-bed column height increasing from 5 to 10 cm (corresponding HPA of 0.35 and 0.68 g, GO of 0.33 and 0.60 g, respectively), resulting in a wider mass transfer zone.

To analyze scientifically, we plotted the diagram between parameter k fitted by Y-N model and temperature(T), and listed the k value above each bar, shown in Fig. 10. It can be discerned that with the increase of temperature, k value increased linearly, inferring the higher mass transfer rate because of higher diffusion rate of VOCs molecules to the adsorbent sites. Generally, there mainly exist three mass transfer resistances effecting the adsorption process: external film resistance, macropore and mesopore resistance, and micropore resistance. The pore resistances demonstrated

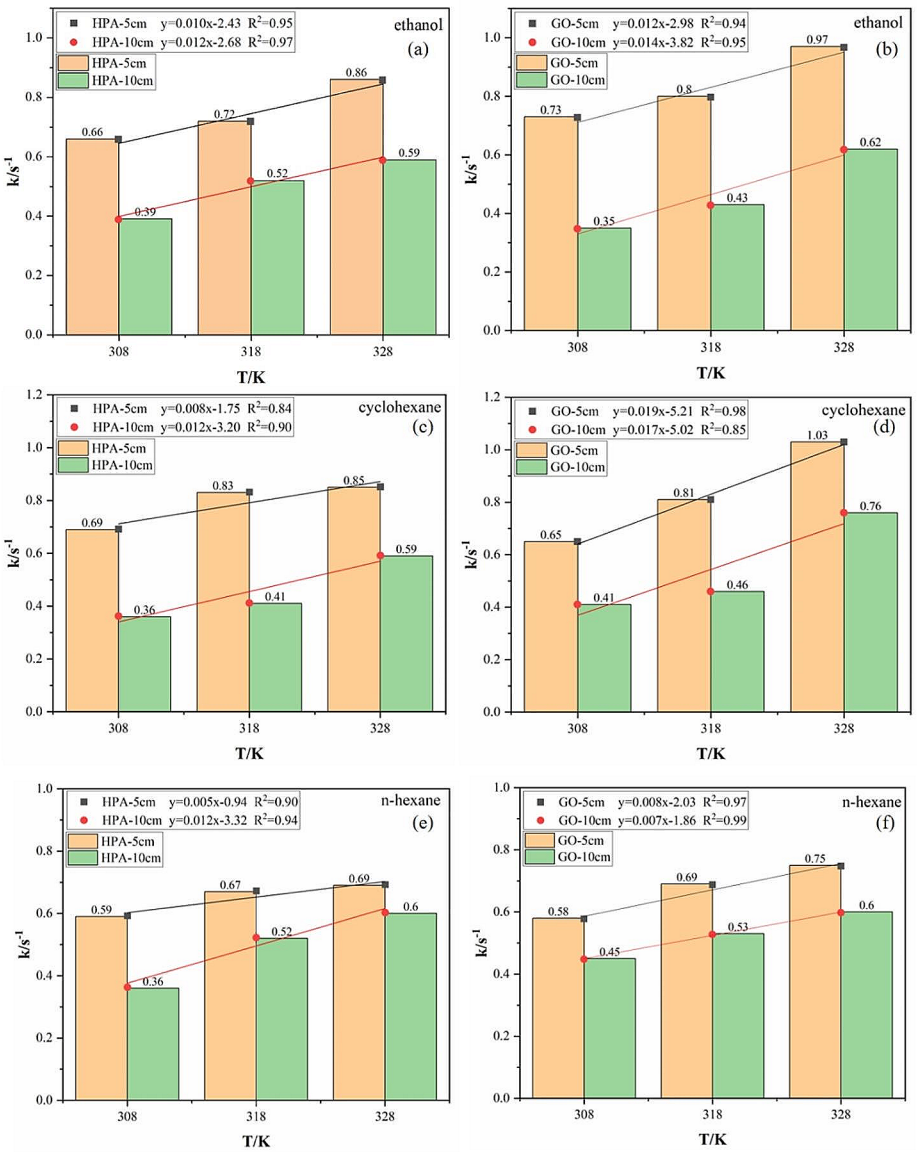

Fig. 10 Dynamic adsorption rate of VOCs at different temperatures with different adsorbent column height

strong dependence on temperature while the external film resistance shows only little temperature dependence [9]. Hence, during dynamic adsorption process of ethanol, n-hexane and cyclohexane on HPA and GO at different temperature, the main mass transfer resistances were pore resistances.

3.3.1 Effect of VOCs and adsorbent properties

As for the three VOCs on the same adsorbent, the *k* value were approximate, illustrating that the physical properties of ethanol, n-hexane and cyclohexane have little influence on mass transfer in this paper. Furthermore, for n-hexane and cyclohexane, the *k* values were similarity on HPA and GO. While for the ethanol, the *k* value on GO were slightly higher than the *k* value on HPA, indicating that the mass transfer resistance on GO were lower than HPA for ethanol adsorption. As mentioned above, GO have a higher affinity to ethanol than HPA, contributing to higher adsorption rate. Therefore, all these results make it clear that GO is a good alternative adsorbent for VOCs recovery.

3.3.2 Effect of column height

In addition, it should be noted in Fig. 10 that the adsorption diffusion rate *k* of three VOCs on HPA and GO were significantly lower for H = 10 cm. This is a consequence of higher flow resistance at higher column height [22]. Further, from the linear relationship plot between *k* value and temperature in Fig. 10, we could know that the slope value had no regular trend with different column height. Hence, in accord with dynamic adsorption capacity, the effect of temperature on adsorption rate was also relatively independent with column height.

4 Conclusion

In this paper, the dynamic adsorption of ethanol, n-hexane, and cyclohexane on graphene oxide was investigated at temperatures of 308 K, 318 K, and 328 K in comparison with hypercrosslinked polymeric adsorbent.

(1) The breakthrough adsorption time and capacity of ethanol, n-hexane and cyclohexane on two adsorbents were as follows: ethanol > cyclohexane > n-hexane, related with physical parameters of VOCs. But the physical properties of ethanol, n-hexane and cyclohexane have little influence on dynamic adsorption rate in this paper.

(2) For n-hexane and cyclohexane, their breakthrough adsorption capacity on HPA were higher than that on GO, but their *k* values were similarity on HPA and GO. While for ethanol, the breakthrough capacity and *k* value on GO were higher than HPA. In addition, the negative effect of temperature on VOCs adsorption on GO was lower than HPA. Therefore, GO is a good alternative adsorbent for VOCs recovery.

(3) With higher column height, the dynamic adsorption capacity was higher but the adsorption rate was lower. But the negative influence of temperature on dynamic adsorption capacity and rate were relative independent with column height of adsorbent.

Acknowledgements This research was financially funded by the National Science Foundation for Young Scientists of China (Grant No. 51808485), Research Project Supported by Shanxi Scholarship Council of China (Grant No. 2021 – 150) and Yuncheng University (YQ-2022011).

Author contributions Lijuan Jia (First Author, Corresponding Author) contributed to overall idea, writing, and research. Mingxuan Yang and Xiangbin Shen contributed to the adsorption experiment and data collecting; Yuying Zhang, Dan Luo and Yangping Zhang contributed to the data analysis and editing. All authors reviewed the manuscript and approved the submitted version.

Data availability All data generated or analyzed during this study are included in this article.

Declarations

Consent for publication The authors attest that the contents in the manuscript have not been previously published or offered for publication elsewhere.

Conflict of interest The authors declare no competing interests.

References

1 Akubuiro, E.C.: Potential mechanistic routes for the oxidative disintegration of ketones on carbon adsorbents. Ind. Eng. Chem. Res. **32**(12), 2960–2968 (1993)
2 Alzate-Sań chez, D.M., Smith, B.J., Alsbaiee, A., Hinestroza, J.P., Dichtel, W.R.: Cotton Fabric Functionalized with a betaCyclodextrin Polymer Captures Organic Pollutants from Contaminated Air and Water. Chem. Mater. 28, 8340 – 8346 (2016)
3 Bae, J.S., Do, D.D.: On the equilibrium and dynamic behavior of alcohol vapors in activated carbon. Chem. Eng. Sci. **61**, 6468–6477 (2006)
4 Balandin, A.A., Ghosh, S., Bao, W., Calizo, I., Teweldebrhan, D., Miao, F., Lau, C.N.: Superior thermal conductivity of single-layer graphene. Nano Letter. **8**, 902–907 (2008)
5 Boehm, H.P.: Some aspects of the Surface Chemistry of Carbon Blacks and other carbons. Carbon. **32**, 759–769 (1994)
6 Crini, G.: Non-conventional low-cost adsorbents for dye removal: A review. Bioresource Technol. **97**(9), 1061–1085 (2006)
7 Dai, Y., Li, M., Liu, F., Xue, M., Wang, Y.Q., Zhao, C.C.: Graphene oxide wrapped copper-benzene-1,3,5-tricarboxylate metal organic framework as efficient absorbent for gaseous toluene under ambient conditions. Environ. Sci. Pollut Res. **26**, 2477–2491 (2019)
8 Dawson, R., Cooper, A.I., Adams, D.J.: Nanoporous organic polymer networks. Prog Polym. Sci. **37**(4), 530–563 (2012)

9 Fogler, H.S.: Elements of Chemical Reaction Engineering. Prentice Hall, Englewood Cliffs, NJ (1986)
10 Fontanals, N., Marcé, R.M., Borrull, F., Cormack, P.A.G.: Hypercrosslinked materials: Preparation, characterisation and applications. Polym. Chem. **6**(41), 7231–7244 (2015)
11 Fuertes, A.B., Marban, G., Nevskaia, D.M.: Adsorption of volatile organic compounds by means of activated carbon fiber-based monoliths. Carbon. **41**, 87–96 (2003)
12 Gurani, K.B., Mise, S.R.: Fixed Bed Modelling Column Adsorption studies by activated Carbon for removal of Fluoride. Ecol. Environ. Conserv. **28**(3), 1446–1451 (2022)
13 Huang, Z., Kang, F., Liang, K., Hao, J.: Breakthrough of methyethylketone and benzene vapors in activated carbon fiber beds. J. Hazard. Mater. **B98**, 107–115 (2003)
14 Jia, L., Yu, W., Long, C., Li, A.: Adsorption equilibrium and dynamics of gasoline vapors onto polymeric adsorbents. Environ. Sci. Pollut Res. **21**, 3756–3763 (2014)
15 Jia, L., Song, X., Wu, J., Long, C.: Surface properties of Hyper-Cross-linked Polymeric resins using Inverse Gas Chromatography: Effect of Post-cross-linking solvents. J. Phys. Chem. C. **119**, 21404–21412 (2015)
16 Jia, L., Ma, J., Shi, Q., Long, C.: Prediction of adsorption equilibrium of VOCs onto hyper-cross-linked polymeric resin at environmentally relevant temperatures and concentrations using inverse gas chromatography. Environ. Sci. Technol. **51**(1), 522–530 (2017)
17 Jia, L., Shi, Q., Xie, S., Long, C.: Effect of Pre-adsorbed Water in Hydrophobic Polymeric Resin on Adsorption equilibrium and breakthrough of 1, 2-Dichloroethane. Adsorption. **24**, 73–80 (2018)
18 Jia, L., Niu, B., Wu, Y., Jing, X.: Predicting the adsorption of indoor VOCs onto commercial activated Carbon based on Linear Solvation Energy Relationship. J. Environ. Eng. **146**(10), 04020113 (2020)
19 Kane, A., Giraudet, S., Vilmain, J.B., Cloirec, L.: Intensification of the temperature-swing adsorption process with a heat pump for the recovery of dichloromethane. J. Environ. Chem. Eng. **3**(2), 734–743 (2015)
20 Kyzas, G.Z., Deliyanni, E.A., Bikiaris, D.N., Mitropoulos, A.C.: Graphene composites as dye adsorbents. Rev. Chem. Eng. Res. Des. **129**, 75–88 (2018)
21 Lillo-Ro´denas, M.A., Cazorla-Amoro´s, D., Linares-Solano, A.: Behavior of activated carbons with different pore size distributions and surface oxygen groups for benzene and toluene adsorption at low concentrations. Carbon. **43**, 1758–1767 (2005)
22 Lin, X.Q., Huang, Q.L., Qi, G.X., Shi, S.L., Xiong, L., Huang, C., Chen, X.F., Li, H.L., Chen, X.D.: Estimation of fixed-bed column parameters and mathematical modeling of breakthrough behaviors for adsorption of levulinic acid from aqueous solution using SY-01 resin. Sep. Purif. Technol. **174**, 222–231 (2017)
23 Liu, P., Long, C., Li, Q.F., Qian, H.M., Li, A.M., Zhang, Q.X.: Adsorption of trichloroethylene and benzene vapors onto hypercrosslinked polymeric resin. J. Hazard. Mater. **166**(1), 46–51 (2009)
24 Liu, B., Zeng, L., Mao, J., Ren, Q.: Simulation of levulinic acid adsorption in packed beds using parallel pore/surface diffusion model. Chem. Eng. Technol. **33**, 1146–1152 (2010)
25 Long, C., Li, Y., Yu, W.H., Li, A.M.: Removal of benzene and methyl ethyl ketone vapor: Comparison of hypercrosslinked polymeric adsorbent with activated carbon. J. Hazard. Mater. **203**, 251–256 (2012)
26 Lorimier, C., Subrenat, A., Le Coq, L., Le Cloirec, P.: Adsorption of toluene onto activated carbon fibre cloths and felts: Application to indoor air treatment. Environ. Technol. **26**(11), 1217–1230 (2005)
27 Menard, D., Py, X., Mazet, N.: Activated carbon monolith of high thermal conductivity for adsorption processes improvement part A: Adsorption step. Chem. Eng. Process. **44**, 1029–1038 (2005)
28 Mohammed, N., Grishkewich, N., Waeijen, H.A., Berry, R.M., Tam, K.C.: Continuous flow adsorption of methylene blue by cellulose nanocrystal-alginate hydrogel beads in fixed bed columns. Carbohyd Polym. **136**, 1194–1202 (2016)
29 Shafeeyan, M.S., Daud, W.M.A.W., Shamiri, A., Aghamohammadi, N.: Modeling of carbon dioxide adsorption onto ammonia-modified activated carbon: Kinetic analysis and breakthrough behavior. Energ. Fuel. **29**, 6565–6577 (2015)
30 Shim, W.G., Lee, J.W., Moon, H.: Adsorption equilibrium and column dynamics of VOCs on MCM-48 depending on pelletizing pressure. Micro Meso Mater. **88**, 112–125 (2006)
31 Virtanen, A., Joutsensaari, J., Koop, T., Yli-Pirila, P.: An amorphous solid state of biogenic secondary organic aerosol particles. Nature. **467**(7317), 824–827 (2010)
32 Widjaja, H., Altarawneh, M., Jiang, Z.T.: Trends of elemental adsorption on graphene. Can. J. Phys. **94**(5), 437–447 (2016)
33 Wood, G.O.: Affinity coefficients of the Polanyi/Dubinin adsorption isotherm equations - a review with compilations and correlations. Carbon. **39**, 343–356 (2001)
34 Wu, C.Y., Chung, T.W., Yang, T.C.K., Chen, M.T.: Dynamic determination of the concentration of volatile alcohols in a fixed bed of zeolite 13X by FT-IR. J. Hazard. Mater. **B137**, 893–898 (2006)
35 Wu, J., Jia, L., Wu, L., Long, C., Deng, W., Zhang, Q.: Prediction of the breakthrough curves of VOC isothermal adsorption on hypercrosslinked polymeric adsorbents in a fixed bed. RSC AdV. **6**(34), 28986–28993 (2016)
36 Yoon, Y.H., Nelson, J.H.: Application of gas adsorption kinetics I: A theoretical model for respirator cartridge service life. Am. Ind. Hyg. Assoc. J. **45**(8), 509–516 (1984)
37 Zerbonia, R.A., Brockmann, C.M., Peterson, P.R., Housley, D.: Carbon bed fires and use of carbon canisters for air emissions control on fixed-rooftanks. J. Air Waste Manage. **51**, 1617–1627 (2001)